Submitted to
Proc. of Amer. Soc.
of Civil Engs.

Interactive modeling of surface waves and boundary layer [1]

D. Chalikov[2]

Abstract

A new theoretical approach to investigate the nonlinear wave dynamics and wind-wave interaction is developed on a coupled model of wave boundary layer (WBL) and surface waves dynamics. WBL-model is based on the nonstatic Reynolds equations written in nonstationary conformal surface-following coordinate system in the 2-D domain above an arbitrary periodic moving surface which may be represented by a Fourier series. Closure scheme is based on a full turbulent energy evolution equation. Wave dynamics are simulated based of the equations for potential waves. The solutions for air and water components are coupled at each time step by assimilation of surface pressure (obtained from the boundary layer model) into wave model, and shape of the surface and surface velocity components (obtained from the wave model) into boundary layer model. The method developed may be applied to a broad range of wave dynamics and wind-wave interaction problems where the assumption of two-dimensionality is acceptable.

1. Introduction

Previous investigations of dynamic interaction between wind and waves were performed mostly for idealized cases of steady monochromatic harmonic waves, which were predescribed at the air-sea interface (Gent, Taylor, 1977; Chalikov, 1978, 1986). However, a recently developed method for numerical solution of potential wave equations (Chalikov, Sheinin, 1997) allows the possibility to simulate the long-term evolution of nonstationary surface wave fields. Wave model is based on the basic equations of potential flow with a

[1]OMB contribution Nr. 153.

[2]UCAR Visiting Scientist, Ocean Modeling Branch, National Center for Environmental Prediction, NOAA/NWS, 5200 Auth Road, Room 209, Camp Springs, MD 21746, USA, E-mail: wd20dc@sun1.wwb.noaa.gov

free surface written in confomal surface-following nonstationary coordinates. This model is coupled with Wave Boundary Layer (WBL) model. The WBL is defined as the lowest part of the atmospheric boundary layer above the surface waves the structure of which is directly influenced by wave-produced fluctuations of velocity and pressure. The exchange of momentum, energy and mass between air and water depends considerably on the specific properties of the WBL. Direct empirical data on the statistical structure of the WBL is sparse, and the only viable method of investigating the WBL is through numerical modeling.

2. Coupled model

Let us consider the motion of a two-layer liquid in the domain

$$-\infty < x < \infty, \quad -\infty < y < \infty, \quad -H_w \leq z \leq H_a, \tag{1}$$

with interface $h(x, y, t)$. The origin of coordinate z coincides with the mean level h. Density of liquid in upper part of the domain is $\rho = \rho_a$, and in the lower part is $\rho = \rho_w$. The motion of the surface obeys a kinematic boundary condition

$$w_0 = h_t + u_0 h_x + v_0 h_y, \tag{2}$$

where u_0 and v_0 are velocity components at the surface $z = h$ (subscripts of independent variables denote partial differentiation with respect to the variable.)

A model describing the dynamics of a two-layer liquid is formulated with the following restrictions

1. Surface $h(x, y, t)$ is periodic in x and y directions with period $2\pi L$. Consequently, surface may be represented by Fourier expansion

$$\eta(x, y, t) = \sum h_{k,l}(t)\Theta_{kl}(x, y); \tag{3}$$

where $k = 1, 2, 3..., \infty$ and $l = 1, 2, 3, ...\infty$ are wave numbers in x and y directions, and Θ_{kl} are the basis functions.

2. Direction of x-axis coincides with direction of tangentional force τ apllied at upper boundary of domain $z = H_a$. τ is a constant in space and time.

3. Fourier coefficients for the surface obey conditions $h_{kl} = 0$ at $l \leq M$. This condition assumes that up to truncation wave number $k = M$ surface $h(x, y, t)$ may be considered as a one-dimensional in the horizontal domain.

4. Probabilty distributions for surface disturbances and turbulent fluctuations of pressure and velocuty are invariant with respect to parallel shifts and reflection with respect to X-axis.

2.1 Model of boundary layer above waves

Let us consider the conformal surface-following coordinate transformation for upper domain at $\zeta > 0$

$$x = \xi - \sum_{-M \le k \le M, k \neq 0} \eta_{-k}(\tau) \frac{\cosh k(\tilde{H}_a - \zeta)}{\sinh k\tilde{H}_a} \vartheta_k(\xi), \tag{4}$$

$$z = \zeta + \eta_0(\tau) + \sum_{-M \le k \le M, k \neq 0} \eta_k(\tau) \frac{\sinh k(\tilde{H}_a - \zeta)}{\sinh k\tilde{H}_a} \vartheta_k(\xi), \tag{5}$$

where η_k are the coefficients of Fourier expansion of the free surface $\eta(\xi, \tau)$ with respect to the new horizontal coordinate ξ, and ϑ_k denotes the function

$$\vartheta_k(\xi) = \begin{cases} \cos k\xi & k \ge 0 \\ \sin k\xi & k < 0, \end{cases} \tag{6}$$

(note that $(\vartheta_k)_\xi = k\vartheta_{-k}$, and $\sum (A_k \vartheta_k)_\xi = -\sum k A_{-k} \vartheta_k$); M is the truncation wavenumber to be used in numerical integration.

Euler equations after transformation and averaging (Chalikov, 1978) can be expressed as (signs of averaging for first order moments are omitted)

$$\frac{dJu}{d\tau} = -\frac{\partial p x_\xi}{\partial \xi} + \frac{\partial p z_\xi}{\partial \zeta} - \frac{\partial (x_\xi \overline{u'u'} + z_\xi \overline{u'w'})}{\partial \xi} - \frac{\partial (-z_\xi \overline{u'u'} + x_\xi \overline{u'w'})}{\partial \zeta}, \tag{7}$$

$$\frac{dJw}{d\tau} = -\frac{\partial p z_\xi}{\partial \xi} - \frac{\partial p x_\xi}{\partial \zeta} - \frac{\partial (z_\xi \overline{u'w'} + x_\xi \overline{w'w'})}{\partial \xi} - \frac{\partial (-z_\xi \overline{u'w'} + x_\xi \overline{u'w'})}{\partial \zeta}, \tag{8}$$

where $\frac{d}{dt}$ denotes a total time derivative

$$\frac{dJ()}{d\tau} = \frac{\partial J()}{\partial \tau} + \frac{\partial J\mathbf{u}()}{\partial \xi} + \frac{\partial J\mathbf{w}()}{\partial \zeta}, \tag{9}$$

The continuity equation becomes

$$\frac{\partial J}{\partial \tau} + \frac{\partial J\mathbf{u}}{\partial \xi} + \frac{\partial J\mathbf{w}}{\partial \zeta} = 0. \tag{10}$$

Equations (7)-(8) are written in nondimensional form, with the following scales: length L, time $\mathcal{T} = L^{1/2} g^{-1/2}$, velocity $L^{1/2} g^{1/2}$, pressure $\mathcal{P} = \rho_a g L$ (g is acceleration of gravity).

In equations (7-10), J is a Jacobian of the transformation given by (4),(5):

$$J = x_\xi^2 + z_\xi^2 = x_\zeta^2 + z_\zeta^2, \tag{11}$$

and $\mathbf{u}$, $\mathbf{w}$ are the contravariant velocity components

$$\mathbf{u} = J^{-1}((u - x_\tau)x_\xi + (w - z_\tau)z_\xi) \tag{12}$$

$$\mathbf{w} = J^{-1}(-(u - x_\tau)z_\xi + (w - z_\tau)x_\xi) \tag{13}$$

On the interface $\xi = 0(z = \eta)$ the velocity components obey kinematic condition (2), which in (ξ, ζ)-coordinates takes the form

$$-(u - x_\tau)z_\xi + (w - z_\tau)x_\xi = 0. \tag{14}$$

Hence, the vertical component of contravariant velocity $\mathbf{w}$ is equal to zero on a surface. It means that momentum and any other properties are not transferred through the surface by velocity field.

Second order turbulence moments are traditionaly represented as product of turbulent viscosity coefficient K and correspondent component of strain velocity tenzor $\Phi_{i,j}$

$$\overline{u'u'} = 2KJ^{-1}\Phi_{11} = 2KJ^{-1}\left(\frac{\partial u x_\xi}{\partial \xi} - \frac{\partial u z_\xi}{\partial \zeta}\right) \tag{15}$$

$$\overline{u'w'} = KJ^{-1}\Phi_{12} = KJ^{-1}\left(\frac{\partial (u z_\xi + w x_\xi)}{\partial \xi} + \frac{\partial (u x_\xi - w z_\xi)}{\partial \zeta}\right) \tag{16}$$

$$\overline{w'w'} = 2KJ^{-1}\Phi_{22} = 2KJ^{-1}\left(\frac{\partial w z_\xi}{\partial \xi} + \frac{\partial w x_\xi}{\partial \zeta}\right) \tag{17}$$

Turbulent viscosity coefficient is taken in a form

$$K = kl(c\tau e)^{1/2} \tag{18}$$

where $k = 0.4$ is von-Karman constant, and $c = 4.6$, and e is a normalized kinetic energy of turbulence

$$e \equiv \frac{1}{2}(\tau c)^{-1}\left((u')^2 + (w')^2 + (v')^2\right) \tag{19}$$

Turbulent lenght scale l was calculated through the relation

$$l = k\int_0^\zeta J d\zeta \tag{20}$$

which generalizes a routine mixing length relation $l = kz$.

Turbulent energy is calculated with evolutionary equation

$$\frac{dJe}{d\tau} = \frac{\partial}{\partial \xi}K\frac{\partial e}{\partial \xi} + \frac{\partial}{\partial \zeta}K\frac{\partial e}{\partial \zeta} + \frac{JK}{2c\tau}\Phi_{ij}\Phi_{ji} - \frac{JKe}{cl^2} \tag{21}$$

Eqns (34) and (35) are written for the surface $\zeta = 0$ (so that $z = \eta$ as represented by expansion (30)), and J is the Jacobian of the transformation.

Coefficients in Fourier expansion of function f in (34) and (35) are connected with coefficients in Fourier expansion of function g by relation

$$f_k = \begin{cases} g_{-k} \coth(k\tilde{H}_w) & \text{if } k \neq 0 \\ \frac{1}{2} \sum_{-M \leq k \leq M, k \neq 0} k\eta_{-k} g_k \sinh^{-2}(k\tilde{H}_w) & \text{if } k = 0 \end{cases} \tag{37}$$

Boundary condition (27) readily yields:

$$\Phi_\zeta(\xi, \zeta = -\tilde{H}_w, \tau) = 0. \tag{38}$$

The Laplace equation (33) with boundary condition (38) is solved via Fourier expansion (which reduces system (33) – (35) to a 1-D problem):

$$\Phi = \sum_{-M \leq k \leq M} \phi_k(\tau) \frac{\cosh k(\zeta + \tilde{H}_w)}{\cosh k\tilde{H}_w} \vartheta_k(\xi), \tag{39}$$

where ϕ_k are Fourier coefficients of the surface potential $\Phi(\xi, \zeta = 0, \tau)$. Equations eqns (34–36) together with definition of (11) constitute a closed system of equations for the surface functions $z(\xi, \zeta = 0, \tau) = \eta(\xi, \tau)$ and $\Phi(\xi, \zeta = 0, \tau)$. Thus, the original system of equations (22), (24) is transformed **without any simplifications** into two simple nostationary equations which can be effectively solved using the Fourier transform method (see details in Chalikov, Sheinin, 1997).

2.3 Boundary conditions and matching through the interface

We assume that height of air domain H_a is chosen large enough, so that wave-produced fluctuations at $z = H_a$ may be neglected. Natural boundary conditions in this case are assigning the horizontal component of the vertical flux of momentum, zero vertical velocity, and absence of wave-produced perturbation of turbulent energy. That is

$$z = \zeta = H_a: \quad \overline{u'w'} = \tau, \quad w = 0, \quad e = 1. \tag{40}$$

Lower boundary condition (38) has been alreday taken into account in expansion for velocity potential (39). Surface pressure p_0 which is calculated in the boundary layer model is taken into account in equation (35). Influence of waves on the boundary layer is accounted through the metric coefficients x_τ, z_τ, x_ξ, z_ξ included in Eqs. (7 – 13) and boundary conditions on interface $h(x,t)$. Because a wave model is based on potential flow assumption cannot assimilate a surface tangential stress, matching conditions on interface consist of the continuity of velocities (u, w) and pressure p. Linear theory (Mails,

1955) gives an estimate for Fourier coefficients of the pressure field $p_k \sim \beta\eta_k$ ($\beta \sim 10^{-3} - 10^{-3}$ is à wind-wave interaction parameter). Because term ϵp is small, matching of water and air models may be performed by independent integration of both problems with exchange of matching information at each time step. A primary boundary condition for boundary layer on an interface $\zeta = 0$ ($z = h(x,t)$) is assigning the surface velocity components $u_0(\xi,\tau)$ and $w_0(\xi,\tau)$ calculated in a wave model. Nevertheless, this condition is diffucult to use in the air model directly because the tangentional component of velocity has a logarithmic singularity; thus, the vertical step in the vicinity of surface should be on the order of roughness parameter z_0. This problem may be effectively resolved by assuming that, very close to the surface in a layer with the height of h_r, the structure of flow is fully adjusted to local tangentional stress τ_0, which obeys the quadratic law

$$\tau_0 = C_l J_0(\mathbf{u} - \mathbf{u}_0) \mid \mathbf{u} - \mathbf{u}_0 \mid . \tag{41}$$

Here $\mathbf{u}$ is contravariant u-component of velocity at height h. $\mathbf{u}_0$ is its value on the surface calculated by (12), (13), with surface velocity component in the water model given by

$$u_0 = J^{-1}(\Phi_x x_\xi - \Phi_\zeta z_\xi) \tag{42}$$

$$w_0 = J^{-1}(\Phi_x z_\xi - \Phi_\zeta x_\xi) \tag{43}$$

Thus, stresses are calculated by the relations

$$\overline{u'w'}x_\xi - \overline{w'w'}z_\xi = -\tau_0 x_\xi(0) J_0^{1/2} \tag{44}$$

$$uwz_\xi + \overline{w'w'}x_\xi = -\tau_0 z_\xi(0) J_0^{1/2} \tag{45}$$

We assume that local drag coefficient is connected with roughness parameter ζ_0 defined by energy of subgrid waves.

$$z_0 \sim \left(\int_M^\infty \int_M^\infty S(k,l) dk dl \right)^{1/2} \tag{46}$$

where $S(k,l)$ is two-dimensional wavenumber spectrum of subgrid waves.

It was shown (Chalikov (1996) that z_0 may be estimated by relation

$$z_0 = \chi \alpha^{1/2} \tau \tag{47}$$

where α is a coefficient in the power spectrum in the high frequaency range $S = \alpha\omega^-5$ which is a weak function of wave age (Chalikov, 1996). and χ is a constant of order of 0.1. Note that model results are not very sensitive to value of $\xi\alpha^{1/2}$. Finally, a local drag coefficient is calculated by the relation

$$C_l = \left(\frac{k}{\ln\left(\frac{h_r}{z_0}\right)} \right)^2 \tag{48}$$

where h_τ is the height of adjusted layer which is assumed to be equal to half the thickness of lowest layer in a numerical model.

Assumption on existence of adjusted surface layer is also used for modifications of differential production term P_0 (next to last terms in Eq. (21) in the lowest layer of numerical model.

Matching of models was performed by exchange of information between its air and water counteparts: air model assimilates the geometrical characteristics of the surface $\eta = z(0)$, $\eta_\xi = z_\xi(0)$, $\eta_\tau = z_\tau(0)$ and surface potential $\Phi_0 = \Phi(0)$, and water model assimilated surface pressure p_0. Transfer of data from lower coodinate $\xi(\zeta = 0)$ to upper coordinate $\xi(\zeta > 0)$ was made by cubic splain interpolation of gridded data which provided accuracy of order of 10^{-10}.

3 Numerical scheme

Numerical solution of water and air problems was based on Fourier-grid method, developed initially for modeling of global atmoshere (Orszag, 1970; Eliassen *et al.*, 1970). In order to approximate the derivatives of any variable a over ξ, both in water and air, the spectral method was based on Fourier expansion of the variables with a finite truncation number M.

$$a(\xi, \tau) = \sum_{-M \le k \le M} a_k(t)\vartheta_k(\xi) \tag{49}$$

This expansion was used for calculation of derivatives over ξ for variables x and z in water model and for u_j, v_j and p_j at each level $j = 1, 2, 3, ...L$ in the air model. This presentation allows a calculation of the derivatives over ξ exactly. The nonlinear terms are calculated with the so-called transform method i.e., by their evaluation on a spatial grid. If $Y(u(\xi), v(\xi), w(\xi), ...)$ is a nonlinear function of its arguments which are represented by their Fourier expansions, gridpoint values $u(\xi^{(j)})$, $v(\xi^{(j)})$, $w(\xi^{(j)})$,... are first calculated, i.e., inverse Fourier transforms are performed; then $Y^{(j)} = Y(u(\xi^{(j)}), v(\xi^{(j)}), w(\xi^{(j)}), ...)$ are evaluated at each gridpoint; finally, the Fourier coefficients Y_k of the function Y are found by direct Fourier transform. Here $\xi^{(j)} = 2\pi(j-1)/N$, and N is the number of gridpoints. For precise calculation of nonlinearities we must choose $N > (\nu + 1)M$ where ν is the maximum order of the nonlinearities. Since the equations include division by the Jacobian, the nonlinearity is of infinite order so that, strictly, the above condition on N cannot be met. However, numerical integrations show that if we choose a value of N that ensures an exact evaluation of the cubic nonlinearities ($\nu = 3$), a further increase in N (with fixed M) virtually does not impact the numerical solution (Chalikov, Sheinin, 1996). For most runs, $M = 100$ and $N = 400$ were used.

The vertical derivatives in WBL model were approximated with second-order accuracy on nonuniform grid with vertical step Δz_j growing with z as z^s (s is a stretching parameter). Number of layers L was chosen 30, and $s = 0.5$.

The approximation the differential terms is more or less straightforward.

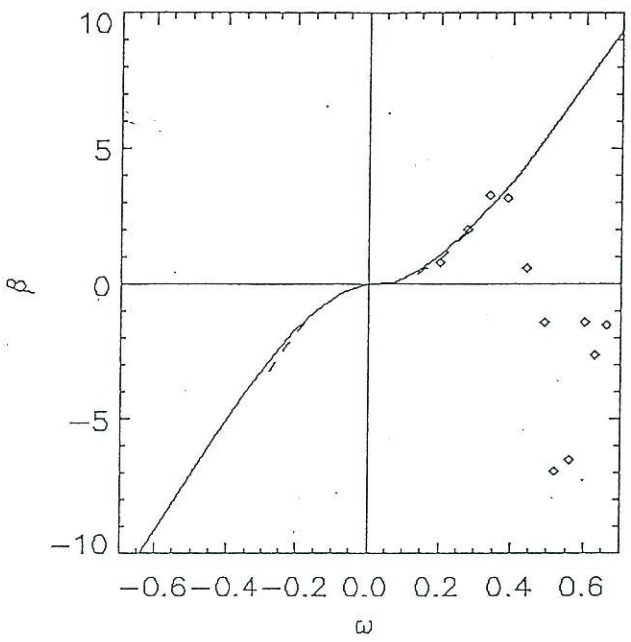

Figure. 1 β-parameter as function of nondimensional frequency: solid line - present model, dashed line - approximation obtained in (Chalikov, 1993). Diamonds are β-function calculated with present model for multi-mode wave field.

where h_k, h_{-k}, P_k, P_{-k}, τ_k, τ_{-k}, $\mathbf{u}_k, \mathbf{u}_{-k}$ are Fourier amplitudes of elevation h and surface pressure p, tangentional stress τ_0, and contravariant u-component of velocity respectively.

As seen, β-function calculated with present model agrees well with results obtained in previous versions of the model. This agreement is not surprising, because present boundary layer model is similar to the previous model (Chalikov, 1986), and the only difference is that previous model did not use a conformal mapping.

Coupled simulation of boundary layer and waves was performed for initially assigned multi-mode wave field with random phases for nondimensional friction velocity $v_\star = 0.2$, corresponding to very young wind waves. Time step was equal 0.001, and calculations were performed up to $t = 500$. Typical examples of spatial structure of simulated fields are shown in Fig. 2 and Fig.3. Apparent discontinuity of stream function on the surface is created by large gradients of velocity in the adjusted layer. Positive anomalies of pressure dominate at upwind sides of waves, and negative - at downwind sides. This correlation of slopes and surface air pressure produces the positive flux of energy from wind to waves.

It is interesting that negative anomalies are usually much larger than positive one in their magnitudes, and they are mostly concentrated close to dominant wave peaks. Even for a monochromatic wave such distribution of pressure cannot be presented by single Fourier pressure mode.

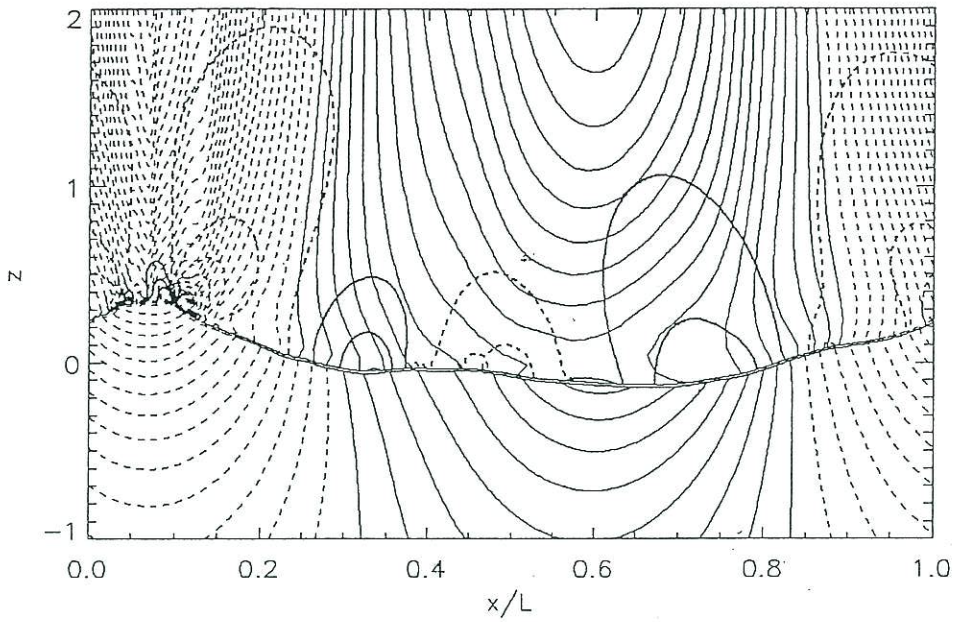

Figure 2. Structure of two-layer flow. Thin lines are contours of stream function of wave motion in water and wave-produced motion in air after removing the mean flow (obtained by averaging in curvilinear coordinates). Thick lines are contours of pressure. For both sets of contours, dashed lines correspond to negative values. Points of breaking are shown by dots in vicinity of wave peak at downwind slope.

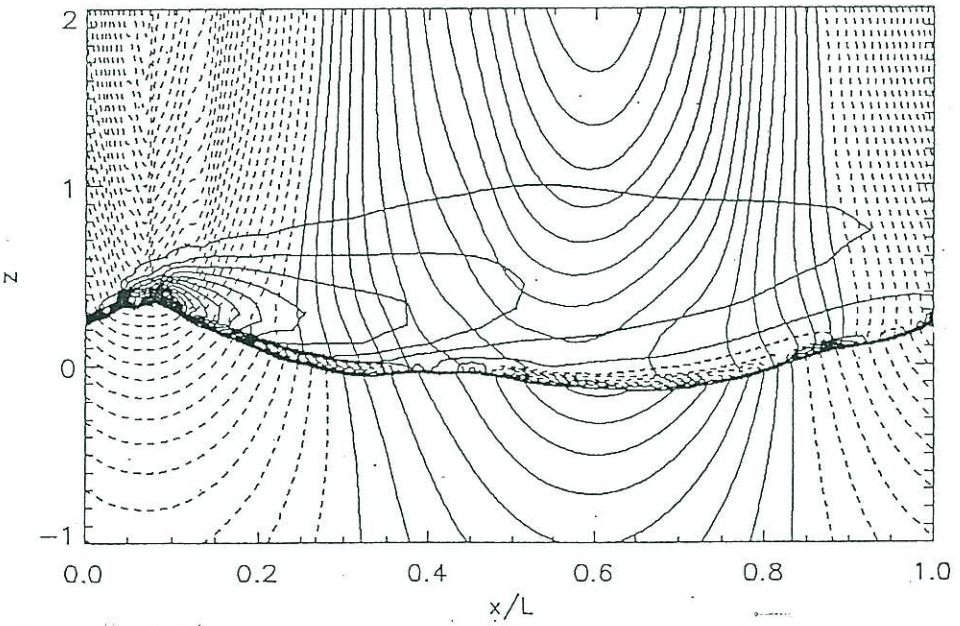

Figure 3. Stream function as in Fig 2 and distribution of $log_{10}e$, Solid lines correspond to positive anomalies of energy of turbulence, and dashed - to negative anomalies.

Consequently, a linear theory of wind-wave interaction cannot be correct. Distribution of energy of turbulence is shown in Fig. 3. As seen, turbulence is enhanced in the vicinity of peaks and weakened along troughs.

Analysis of animations of two-layer flow shows, that deep negative anomalies of pressure and intense generation of turbulence occur simultaneously when a sharp wave peak arises due to specific phase situation. Close to the wave peak, energy of turbulence may increase up to one order of magnitude, forming a stretched plums, which often separates from wave and travels with the flow getting attenuated due to dissipation.

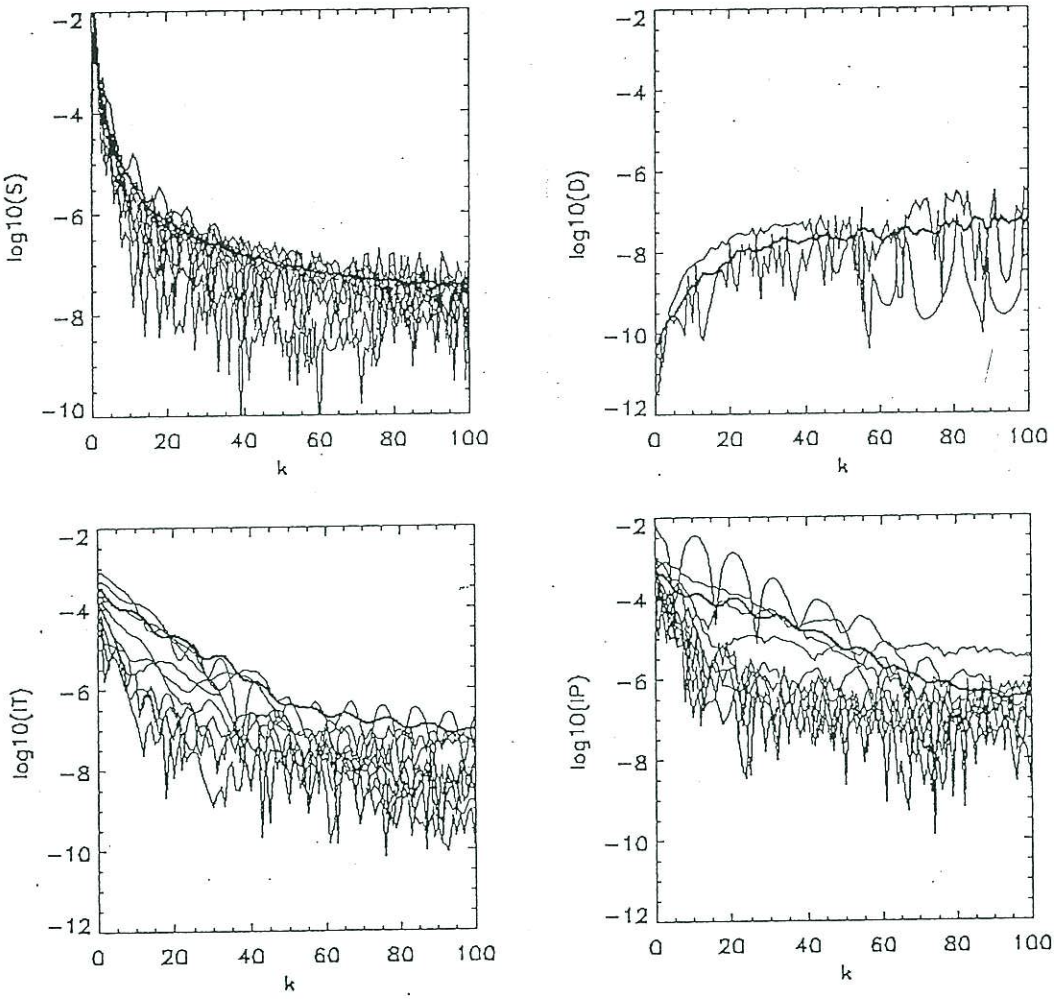

Figure 4. Instataneous wave spectrum (S), Spectrum of dissipation due to breaking (D), Spectrum of Energy flux from wind to waves due to tangential stress (IT) and due to pressure (IP), separated by interval $\delta t = 2$. Thick lines shows averaged spectra.

Spectral characteristics of turbulence are presented in Fig. 4. Variability of wave spectrum increases strongly with wave number. Spectrum density of dissipation is growing with increasing of wave number, and spectrum of input is decreasing. Flux of energy to waves due to pressure field is one order larger than flux of energy due to tangentional stress. Note, that effect of stress cannot be taken into account in potential model of waves. Generally, dissipation of wave energy in this run is much larger than input.

5. Conclusions

In this study, tye dynamical interactions between a wave field on an ocean surface and the atmospheric boundary layer immediately above it are srudied by considering them to be a fully coupled system. A non-stationary conformal surface-following mapping has been developrd to transform the governing potential flow equations for surface waves into two time-dependent differemtial equationswhich are much simpler to deal with, particularly in studies of nonlinear processes. Specifically,, an algorithm has been developed for the parameterization of energy dissipation due to wave breaking. Because the occurance of breaking events depends considerably on phase configuration, this algorithm uses a search for those points in physical space where steepness exceeds a critical value. Dissipation depends mainly on energy flux into high frequency part of the spectrum. The part of the spectrum that contains most of the energy is not much influenced by the critical value of the steepness used.

A conformal mapping used to transform the Reynolds equation in the atmospheric boundary layer above waves. After this transformation, the a second order turbulence closure scheme, based on turbulent energy evolution equation and mixing lengh scale has been used. The WBL Oregion of the atmosheric boundary layer above the ocean surface waves) model was coupled to the wave model through matching the pressure and velocity fields at the interface. For monochromatic waves, the wind-wave interaction parameter is reasonably close to previously known results. But even in this case, the mechanism of overflow is essentially nonlinear and the time scale for reaching equlibrium regime is larger than the period of waves.

The statistical structure of WBL and interaction parameters has been examined. It is shown that dependence of wind-wave interaction parameter on wave number differs from that obtained by considering only monochromatic wave components.

The technique developed can be used to study a variety of nonlinear wave dynamics and nonlinear wind-wave dynamics provided that the twodimensionality in (x, z) and periodicity of waves are accepteptable. Such problems include the investigation of spectral propertioes of nonlinear interactions of

wave field covering a wide range of wave numbers, depths, capillarity coefficients and wind speed. It is also possible to examine the coupling between short and long waves in the absence of wind as well in its presence.

Acknoledgments

Author wish to thank Dr D.B.Rao for reading the manuscript and making many valuable comments.

References

1. Chalikov, D.V. 1978 Numerical simulation of wind-wave interaction. *Journal of Fluid Mech*, **87**, 561 – 582.
2. Chalikov, D.V. 1986 Numerical simulation of the boundary layer above waves. *Bound Layer Met*, **34**, 63 – 98.
Chalikov, D., 1995 The Parameterization of the Wave Boundary Layer. *J. Phys. Oceanogr.*, **25**, 1335 – 1349.
4. Chalikov D. , D. Sheinin . 1997 Direct modeling of one-dimensional nonlinear potential waves. *Advances in Fluid Mechanics. Comp. Mech. Publ.*, 207-258
3. Eliassen, E.B., Machenhauer, B. & Rasmussen, E. 1970 On a numerical method for integration of the hydro-dynamical equations with a spectral representation of the horisontal fields. Report 2, Institute for Teoretisk. Meteorologi, København Universitet, Copenhagen, Denmark.
4. Orszag, S.A. 1970 Transform method for calculation of vector coupled sums. Application to the spectral form of vorticity equation, *Journal of Atmos Sci*, 1970, **27**, 890 – 895.